Worldwide extremely low frequency magnetic field sensor network for sprite studies

Toby Whitley,[1] Martin Füllekrug,[1] Michael Rycroft,[2] Alec Bennett,[3] Frank Wyatt,[4] Don Elliott,[4] Graham Heinson,[5] Adrian Hitchman,[6] Andrew Lewis,[6] Ramotholo Sefako,[7] Pieter Fourie,[7] Jaci Dyers,[7] Alan Thomson,[8] and Simon Flower[8]

Received 16 September 2010; revised 29 April 2011; accepted 11 May 2011; published 12 August 2011.

[1] The first measurements from a new globally distributed extremely low frequency magnetic field sensor network are presented. The recorded data demonstrate that the system observed lightning with continuing currents on a global scale with a timing accuracy of ~30 μs. The network consists of four state of the art instruments at sites in Scotland, the United States, South Africa and Australia. Each instrument records the two horizontal magnetic field components (Bx and By) with a sampling frequency of 4 kHz. The first results show the typical electromagnetic signature of a transient airglow increase (sprite) above a thunderstorm in southern Europe which is simultaneously imaged with a video camera. A similar electromagnetic signature is recorded from a lightning discharge in central Africa, and it is also attributed to a sprite occurrence. Studies using this global network should advance lightning and sprite research considerably.

Citation: Whitley, T., et al. (2011), Worldwide extremely low frequency magnetic field sensor network for sprite studies, *Radio Sci.*, *46*, RS4007, doi:10.1029/2010RS004523.

1. Introduction

[2] Sprites are Transient Luminous Events (TLEs) [*Marshall and Inan*, 2006; *Lyons*, 1996; *Boeck et al.*, 1995; *Franz et al.*, 1990], which occur at heights between 55 and 80 km above large thunderstorms [*Neubert et al.*, 2008; *Füllekrug et al.*, 2006; chap. 14; *Rakov and Uman*, 2003, and references therein; *Sentman and Wescott*, 1993]. Sprites are triggered by intense, typically positive, cloud to ground lightning discharges having a continuing current [*Boccippio et al.*, 1995; *Füllekrug*, 2006; *Rycroft et al.*, 2007] and follow them with a time delay of ~1–100 ms. Sprites and their causative lightning strikes can emit radio waves in the extremely low frequency (ELF) range from ~3 Hz to ~3 kHz although the majority of sprites do not [*Füllekrug et al.*, 2001; *Cummer et al.*, 1998; *Reising et al.*, 1996] and very low frequency (VLF) range [*Rodger et al.*, 1999]. In particular, some sprites and their parent lightning cause a transient excitation of the Earth-ionosphere cavity, or Schumann resonances [*Williams et al.*, 2007; *Rycroft*, 1965], from ~4–50 Hz, which due to the low attenuation at these frequencies [*Taylor and Sao*, 1970] enables a global detection of sprites [*Ignaccolo et al.*, 2006; *Sato and Fukunishi*, 2003; *Füllekrug and Constable*, 2000]. The Sprite Project at the University of Bath has recently deployed a network of four instruments around the world to identify, count and geolocate global sprite occurrences. The gathered data will provide information on the physical properties of sprites in order to assist modeling efforts and will try to improve estimates of global sprite occurrences according to various Planetary Rate of Sprite Events (PROSE) formulas [*Ignaccolo et al.*, 2006; *Chen et al.*, 2008].

[3] The equipment used to make the measurements is the Metronix ADU-07 data logger connected to Metronix MFS-07 induction coils. The equipment records the ELF radio signals generated by lightning discharges and associated radiating sprites [*Huang et al.*, 1999]. The time of arrival difference between the radio signals recorded by the four instruments of the global network can be used to geolocate sprites. To achieve this aim the instrument must be sensitive enough to detect the causative lightning and sprite signal after propagating up to 20 Mm in the Earth-ionosphere waveguide, and accurate enough to provide a suitable temporal measurement for location mapping. Due to the global nature of the network the equipment also has to be remotely accessible and configurable to allow the data to be transferred via the Internet back to the UK for analysis. Furthermore, as well as detecting the sprite and lightning associated Schumann resonances, higher frequencies are recorded to gain more information on the lightning continuing current which triggers sprites and to distinguish the two sources from one another. Three categories of

[1]Department of Electronic and Electrical Engineering, University of Bath, Bath, UK.
[2]CAESAR Consultancy, Cambridge, UK.
[3]Passive Upper Air Sensors R&D, Meteorological Office, Devon, UK.
[4]Scripps Institution of Oceanography, University of California, San Diego, La Jolla, California, USA.
[5]School of Earth and Environmental Sciences, University of Adelaide, Adelaide, South Australia, Australia.
[6]Geoscience Australia, Canberra, ACT, Australia.
[7]South African Astronomical Observatory, Cape Town, South Africa.
[8]British Geological Survey, Edinburgh, UK.

0048-6604/11/2010RS004523

continuing current have previously been identified, very short where the duration was between 3 and 10 ms, short having a duration between 10 and 40 ms, and long where the continuing current lasted in excess of 40 ms [*Saba et al.*, 2010].

[4] Before the global network was deployed the equipment was tested and calibrated in the laboratory and during field tests, including at one of the proposed network sites. The first part of this paper reports the determination of the timing accuracy during these tests. The second part describes the network deployment and the characteristics of the network sites. The third part of the paper reports the first results obtained from the entire network.

2. Equipment

2.1. Data Logger

[5] The data loggers for the project are provided by Metronix Geophysics, part of the Cooper Tools company. The Analogue/Digital Signal Conditioning Unit (ADU-07) consists of a 32-bit processor running Linux on a back board with high-quality 24-bit analog to digital inputs. A GPS clock provides the timing signals to the analog to digital conversion (ADC) boards.

[6] The GPS allows synchronization of multiple ADUs in a network permitting them to be synchronized around the world. The timing signal is taken from the GPS 1 s pulse [*Parkinson and Spilker*, 1996]. The pulse is then averaged over time to provide an increasingly accurate signal that generates an 8 MHz clock signal from which all other timing signals in the ADU is derived. Connectivity to the Internet is provided by a standard 100 Mbit twisted pair (Ethernet) cable. The ADU contains a built-in Web server and the system operation is fully controllable using any standard Web browser. Data is stored on an internal flash disk or on further USB storage devices, including hard drives. The ADU can run off external mains power but typically at a remote site uses one or two 12 V batteries with a power consumption of 3–15 W, depending upon the mode of operation. A maximum of 10 analog inputs with either low-frequency (LF) or high-frequency (HF) sampling can be fitted. The standard configuration is five slots with low-frequency ADC boards working at a maximum data rate of 2048 Hz and five slots for high-frequency boards working at a maximum data rate of 524,288 Hz, with the 24-bit ADC providing a dynamic range greater than 130 dB. The ADU-07 has connections for both magnetic and electric field sensors; however, for the purposes of the Sprite Project only two high-frequency inputs are used. Each input is set to sample one channel at 4 kHz connected to a high-frequency magnetic field sensor.

2.2. Magnetic Field Sensor

[7] The magnetic field sensor (MFS-07) is a high-frequency induction coil magnetometer and two are mounted along the geomagnetic north-south (X) and east-west (Y) axes and connected to each ADU. The magnetic field sensors cover a wide frequency range from 1 mHz up to 50 kHz; they have excellent low noise characteristics (5×10^{-7} nT/$\sqrt{\text{Hz}}$ at 1000 Hz) and a very stable transfer function over temperature and time. The sensors are each factory calibrated using a Solartron 1250 and solenoid then tuned to match one common transfer function, ensuring uniform and consistent performance along with straightforward setup and ease of use. The recorded measurements are corrected for amplitude and phase via the transfer function of the magnetic field sensor. Typical sensitivity of a coil is 0.02 V/(nT*Hz) $f \ll 32$ Hz 0.64 V/nT $f \gg 32$ Hz.

2.3. Calibration and Testing

[8] The initial testing of the ADU took place in the laboratory using a number of generated waveforms including a sine wave, square wave and random noise, all sampled at 4 kHz. In order to test the timing accuracy, two ADU units were needed, both set up to sample the same input signal simultaneously. The time differences between these two measurements should ideally be zero. In reality it will be as close to zero as the GPS clock, hardware accuracy, test conditions and the digital data processing allow. The time difference between two independently recorded time series is determined by the time offset from zero of the interpolated cross covariance function of the two recordings, assuming a finite impulse response of the instrument [*Füllekrug et al.*, 2001]. This technique allows time differences which are smaller than the inverse sampling frequency of the recordings to be found.

[9] Initial tests with a 1 V peak-to-peak sine wave at 30 Hz showed that the ADUs and the subsequent data processing works extremely well as any time differences between the two units were close enough to zero to be undetectable (<0.5 μs). The input was then switched to a 2 V peak-to-peak square wave at 20 Hz to provide a more complex signal. The calculated time differences ranged from zero when the input from the square wave was high to between ±250 μs when the input of the square wave was at a minimum/zero. It was evident that the magnitude of the input signal influences the observed time difference. As a result, a change in the input signal, i.e., an 'event,' was defined when the amplitude increased by 10 mV (signaling the edge of the square wave and peak in the input signal). This event detection reduces the observed time differences to ~2.5 μs (Figure 1, left) and it mimics the deployment situation where a lightning strike likely to cause a sprite would trigger the software to capture it as an event. The time differences were calculated using consecutive sets of four samples which gave the best results when analyzing the measured data. While a greater number of samples provided some averaging of the noise in the system, this did not outweigh the degradation caused by the variations of each sample due to the noise at lower input levels.

[10] This test demonstrates that the calculated timing accuracy between the two data loggers increases with the magnitude of the input signal, but that at lower levels the random noise in the data loggers starts to affect the measureable time differences. This suggests that when the measured signal is small the noise present makes up a greater percentage of the sample and results in decreased timing accuracy.

[11] The next laboratory measurement used randomly generated noise with a bandwidth <5 kHz and an input level of 100 mV peak to peak. This noise source was more similar to the natural signals to be measured (Figure 1, right). It is observed that the calculated timing accuracy of the two

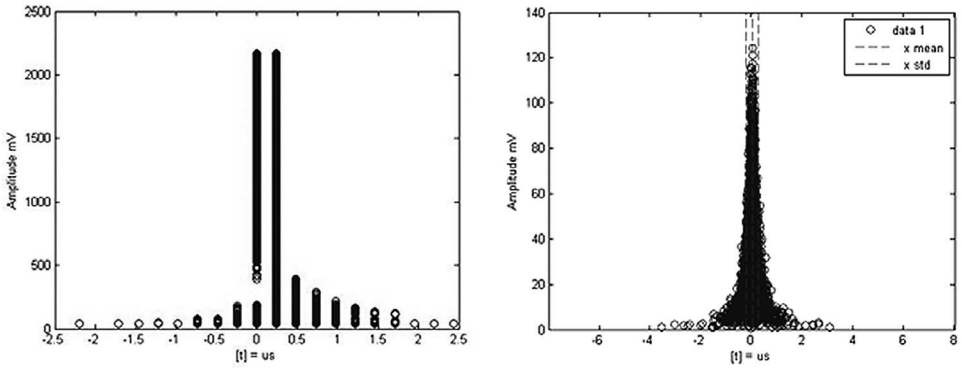

Figure 1. (left) Time differences between two ADUs sampling a 2 V, 20 Hz square wave at 4 kHz. (right) Time differences between two ADUs sampling 100 mV peak-to-peak random noise at 4 kHz.

ADUs increases with increasing magnitude of the input signal. The maximum calculated timing error is ~3 μs.

2.4. GPS Clock Synchronization Test

[12] The final lab test before deployment involved sampling the 1 s pulse from an external GPS clock using all four ADU-07 data loggers to ensure that their clocks were absolutely correct and to determine any hardware delays within the equipment. With the strong pulse from the external GPS no time error could be calculated between the four ADUs. However, all have a consistent positive time delay of 6.836 ms from the 1 s pulse caused by hardware delays within the ADU. This value must be subtracted from the arrival time of any signal measured by the network to enable accurate comparisons with other networks, optical observations and to reduce any errors in calculations of distance to events.

2.5. Field Test

[13] The first field measurements were taken at Wittstock in Germany and involved parallel recordings using two ADUs recording with a sampling frequency of 4 kHz. Each ADU had two MFS-07 coils connected to record real data including lightning and sprite events, as in the deployed network of four stations.

[14] Initially, time differences were calculated for all sampled values with no discrimination for any events. These time differences were greater than those measured under laboratory conditions because the magnitude of the input signal is considerably less and several electromagnetic noise sources were present such as power line harmonic radiation from the mains rail network. The alignment of the coils which was accomplished geomagnetically to an accuracy of ~<1 degree may also have had an effect. In line with the laboratory results, larger input values had greater timing accuracy.

[15] Using software to trigger for ELF events that could be related to sprites and analyzing the timing accuracy for these provides a clearer idea of how good the equipment will be for locating sprites and their causative lightning. Figure 2 shows the time differences between two ADUs for the triggered events. By taking only events that could be sprite related (ELF peaks at 8 and 14 Hz) [*Ogawa and Komatsu*, 2007, 2010] and above a 1 mV threshold at the input, the range of time differences is reduced by a factor of 3. With the triggering level set to give the number of possible events in excess of the number predicted in the literature [*Ignaccolo et al.*, 2006] the standard deviation is ~30 μs which corresponds to a distance error of ~10 km.

[16] One reason for this improvement is that the increased magnitude of the measured signals compared to the background noise gives better performance (as for the laboratory tests). This effect is seen in Figure 1 but more importantly it is also seen in Figure 2 for the results in the field, this shows that the analysis of the recorded data for sprite timing has an accuracy that depends on input signal magnitude, due to SNR considerations.

3. Network Deployment

[17] This section contains a brief description of the magnetic observatory sites around the globe where the data loggers were deployed during July and August 2009. Two sites are presented in more detail; these are the best site, Eskdalemuir, Scotland, because it has the lowest level of

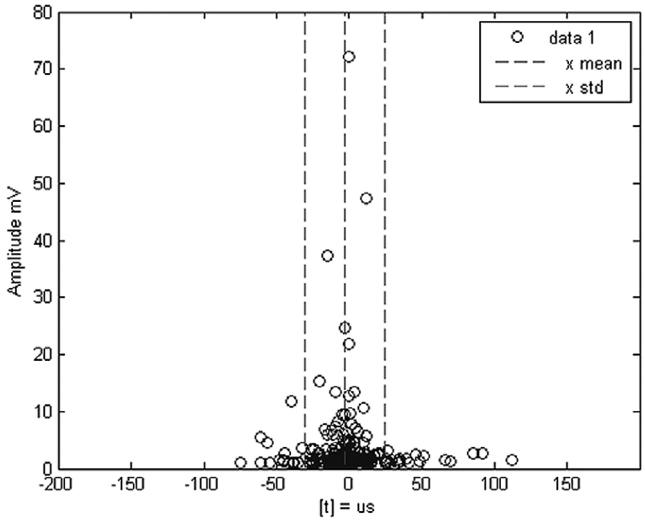

Figure 2. The time differences between two ADUs for 160 triggered events sampling (at 4 kHz) natural signals observed at Wittstock, Germany, between 0930 hr and 1130 hr on 7 July 2008.

Figure 3. The seismic vault entrance at Eskdalemuir, Scotland, with the ADU and sensors behind the hill shown in the inserted photo.

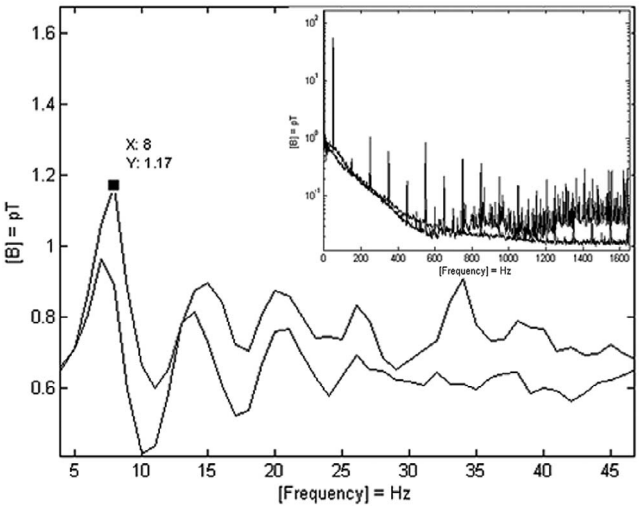

Figure 4. The spectrum at Eskdalemuir, Scotland, exhibits four Earth-ionosphere cavity resonances near 8, 14, 20, and 26 Hz. The inset shows the full spectrum to 1600 Hz recorded from 0821 hr to 0823 hr on 15 June 2009.

power line harmonic radiation and the site with the largest level of power line harmonic radiation, Pinon Flat, California. The observatory sites in Sutherland, South Africa, and Canberra, Australia, are briefly described for completeness. All signals were sampled at 4 kHz. The power spectra are calculated from one second long intervals and are averaged over two minutes to remove random noise. Earth-ionosphere cavity resonances are clearly seen at all sites despite the short time over which the spectra were averaged; usually, averaging over a time of >5 min would be required to see the signals. Previous networks [*Füllekrug et al.*, 2001; *Sato and Fukunishi*, 2003; *Füllekrug and Constable*, 2000; *Chen et al.*, 2008] for detecting and studying lightning and associated sprites have had fewer stations, a smaller dynamic range and lower sampling rates; they did not have the networking capabilities of the ADU-07 data loggers.

3.1. Eskdalemuir, Scotland

[18] The magnetic observatory in Eskdalemuir, Scotland (latitude N 55:17:16, longitude W 3:10:14, elevation 260 m), is run by the British Geological Survey and hosts a UK Meteorological Office observation post. The observatory is 15 miles northeast of Lockerbie with little in the way of surrounding buildings and other possible sources of electromagnetic interference. The ADU is situated 250 m east of a seismic vault on marsh and grassland (Figure 3). The two magnetic sensors are geomagnetically aligned and buried, in gravel, ten meters from the ADU to prevent any vibration or movement in the Earth's natural magnetic field. The sensors are orientated north-south (Hx) and east-west (Hy) using geomagnetic alignment.

[19] Eskdalemuir is electromagnetically the quietest site of the network with the lowest level of 50 Hz power line harmonic radiation at ~50 times the magnitude of the 8 Hz Schumann resonance. Four Earth-ionosphere cavity resonances can readily be distinguished (Figure 4).

3.2. Pinon Flat, California

[20] The Pinon Flat Observatory (latitude N 33:36:36, longitude W 116:27:23, elevation 1276 m) is operated by the Institute of Geophysics and Planetary Physics of the University of California, San Diego. The observatory is situated in the mountains above Palm Desert with a scattering of houses to the west of the site. The underlying rock is granite with up to about 50 cm of broken down rock and sand on the surface. The site suffers from surface floods during heavy rain and does receive occasional lightning strikes. The ADU is housed in the northwest area of the site (Figure 5).

[21] The external power supply for the ADU is housed in a junction box where the optical cable connects directly to the site network. Figure 6 shows the local spectrum at Pinon Flat; four Earth-ionosphere cavity resonances can readily be detected at the site. The inserted graph shows the full spectrum.

[22] Pinon Flat Observatory has the highest level of 60 Hz power line harmonic radiation compared to the other network sites at ~900 times the magnitude of the 8 Hz Schumann resonance. Nevertheless, the large dynamic range of the

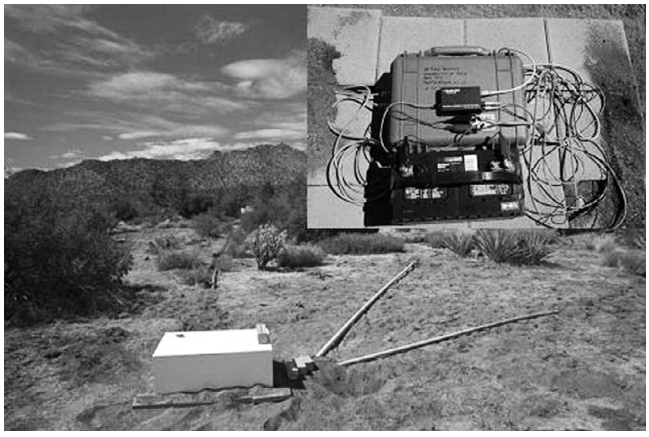

Figure 5. The ADU at Pinon Flat, California, with conduit running northeast and east to the two buried sensors; the inset shows the ADU, 12 V battery, and the fibre to Ethernet media converter.

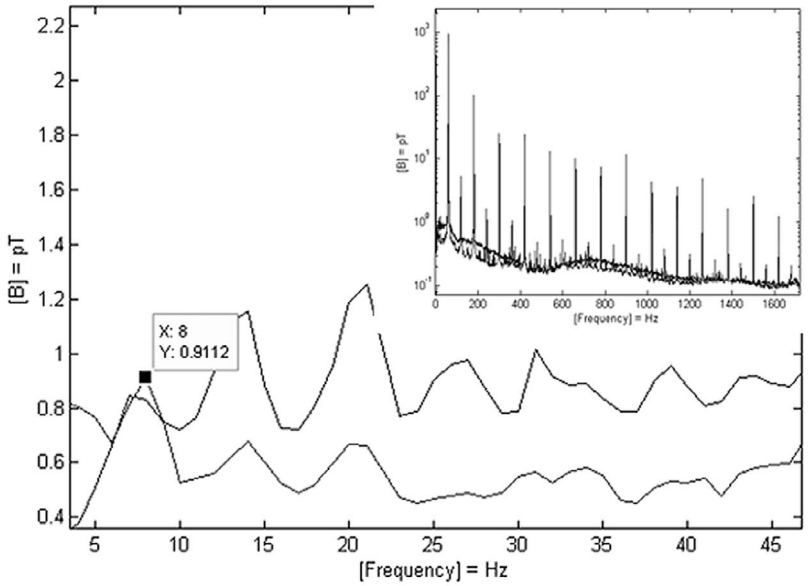

Figure 6. The spectrum at Pinon Flat shows Earth-ionosphere cavity resonances near 8, 14, 20, and 26 Hz. The inset shows the full spectrum to 1600 Hz recorded from 2018 hr to 2020 hr on 8 July 2009.

ADU prevents saturation and no notch filters are needed to detect Earth-ionosphere cavity resonances.

3.3. Canberra, Australia

[23] The site at Canberra, Australia (latitude S 35:18:41, longitude E 149:21:48, elevation 875 m), operated by Geoscience Australia is situated ~30 km east of Canberra. The site has no major buildings within several km and little interference on the site except for local 50 Hz power line harmonic radiation. The ADU is situated in the northwest corner of the site. There is some 50 Hz power line harmonic radiation interference present; this can easily be removed by digital filtering during the data processing. The site is free from other interference, with the possible exception of calibration events using a facility on the site. These calibrations last for a short time (~30 min – 1 h) and can easily be identified by their frequency.

3.4. Sutherland, South Africa

[24] The Sutherland Observatory, South Africa (latitude S 32:22:44, longitude E 20:48:44, elevation 1766 m), is run by the South African Astronomical Observatory, as part of the National Research Foundation. The site is about 300 km northeast of Cape Town. The access point for power and the Internet is in the 1.9 m Radcliffe telescope on the main site. The ADU is 80 m east of this in a rugged plastic housing. The Sutherland instrument records Earth-ionosphere cavity resonances of a similar quality to those of the Eskdalemuir instrument. The rotation of the nearest telescope does not cause any noticeable interference on the recorded data.

4. First Results of the Global Network

[25] After deployment of the global network at the four locations, final adjustments were made to the configurations and settings at each site to allow Internet access and to ensure that each unit was stable (power, connectivity, operating system) for long-term operation. The data quality can be checked via the Internet or if the time of an event is known the waveform can be retrieved for immediate analysis prior to the hard drives from each site being swapped and returned to Bath for full analysis. Bandwidth limitations prevent all of the recorded data being retrieved this way.

[26] The worldwide network of extremely low frequency magnetic field sensors successfully recorded a globally propagating ELF sprite signature at three (the instrument at Eskdalemuir failed to record during this time) of its four stations (Figure 7). The sprite observed over southern Europe on 2 September 2009 at 0307 hr was very bright (Figure 7) and one of 27 recorded and observed over several nights. The electromagnetic recording from the nearest station in South Africa exhibits the continuing current [*Saba et al.*, 2010] from the causative positive cloud to ground lightning discharge and the subsequent radiation from the sprite [*Cummer et al.*, 1998]. This pattern can also be seen at the second nearest site in California, though not with the same clarity. The furthest instrument from the sprite shows only a single peak as much of the high frequencies have been attenuated during propagation in the Earth-ionosphere waveguide.

[27] With data retrieved from all four stations many more globally propagating ELF signatures were found. Waveforms which exhibit a double peak on one or more of the instruments were identified as potential sprite events [*Cummer and Stanley*, 1999]. Using global lightning location data provided by the UK Met Office it can be confirmed that all four instruments recorded the same event. The signature of one such event recorded by the entire worldwide network is shown in Figure 8. The event clearly exhibits a number of sprite associated properties, including lightning continuing current [*Saba et al.*, 2010; *Cummer et al.*, 2006], a double peak from the causative lightning strike and radiating sprite [*Cummer and Stanley*, 1999] at two of the four sites and obviously, global propagation of the ELF

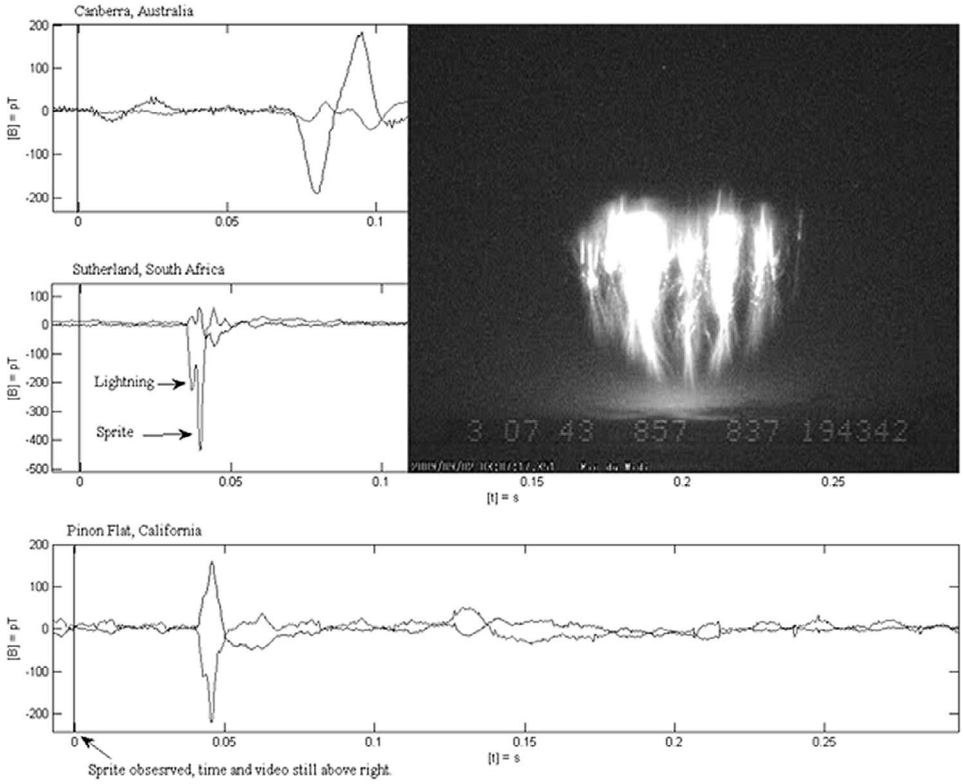

Figure 7. A sprite observed in Europe from the Pic du Midi and recorded along with its parent lightning strike at three of the ADU sites at 0307 hr on 2 September 2009.

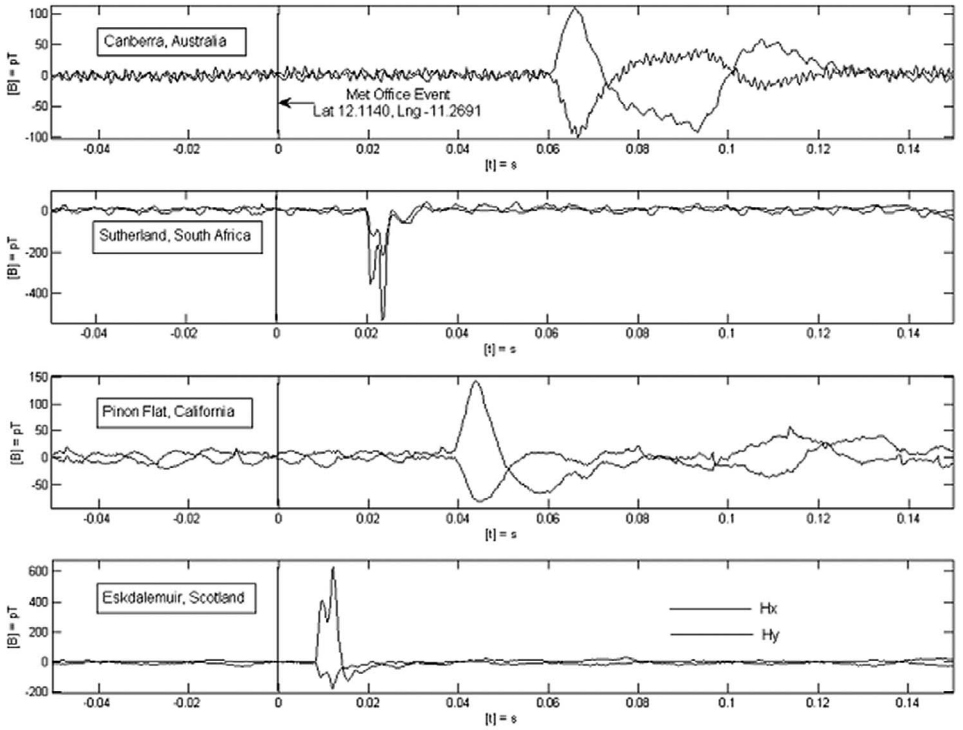

Figure 8. A lightning discharge reported by the British Met Office at 2232 hr on 28 August 2009 and a consecutive sprite recorded at all of the ADU network sites around the world.

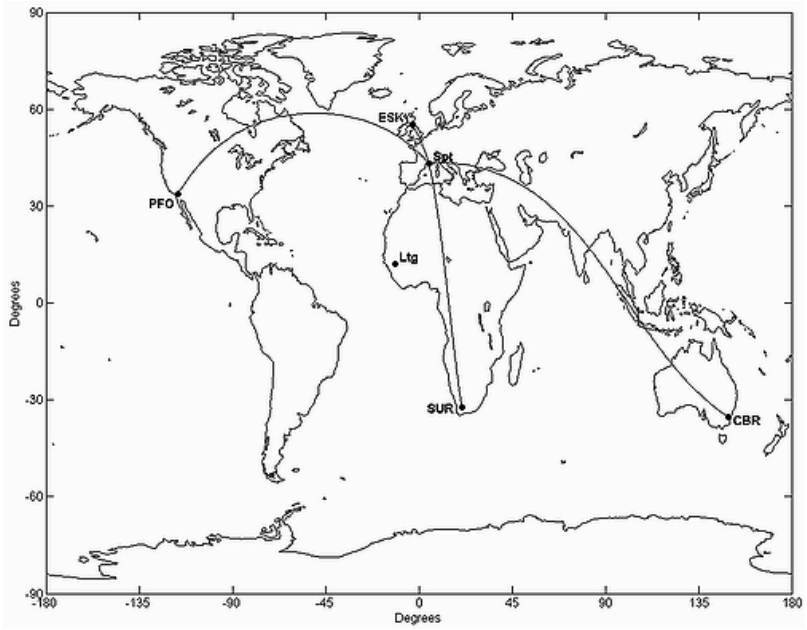

Figure 9. A map of the ADU locations showing the great circles lines from the sprite (spt) observed in Europe on 2 September 2009, and the lightning discharge (ltg) reported by the UK Met Office on 28 August 2009 and recorded by the ADU network showing a potential consecutive sprite (Figure 8).

electromagnetic signature [*Füllekrug et al.*, 2001; *Cummer et al.*, 1998; *Reising et al.*, 1996].

[28] The map in Figure 9 shows the great circle lines from the locations of each ADU measurement site to the location of the sprite observed in Europe (indicated by spt). The map also shows the location of the lightning recorded by the UK Met Office in central Africa (indicated by ltg) which resulted in the probable sprite signature captured by the worldwide ELF network. The two observed events demonstrate that in these examples, the network can record the electromagnetic signatures that have been associated with sprites along with their causative lightning strikes. The network has a high enough temporal resolution that these can be identified as such and detect potential sprites without corresponding optical observations. This will provide further data on the planetary rate of sprite events and allow preliminary global sprite maps to be created. It will also provide information on the physics of sprites for analysis and simulation and modeling work [*Cummer and Inan*, 2000].

5. Discussion

[29] This brand new ELF global network clearly recorded an optically observed sprite in Europe and also an event in central Africa which in all probability generated a sprite. The function of the network is to detect sprite events globally, without the need for optical observations and/or additional data from the UK Met Office or other resources, with a suitable temporal resolution for scientific purposes. A time of arrival difference analysis for ~680 lightning discharges observed 28–30 August 2009 was carried out with the ELF network. To test the operational timing accuracy of the network, the sum of all time differences for each event was calculated (equation (1)). Applying this equation to the events detected gives the distribution in Figure 10 and the overall timing accuracy of the network:

$$(t_1 - t_2) + (t_2 - t_3) + (t_3 - t_4) + (t_4 - t_1) = \Delta t_{12} + \Delta t_{23} + \Delta t_{34} + \Delta t_{41} = \partial t_{sum} \quad (1)$$

This sum, which reflects the accuracy of the networked instruments [*Füllekrug et al.*, 2001], and which is ~30 μs (Figure 10), is in agreement with the calibration and testing of the instruments before the deployment (compare with

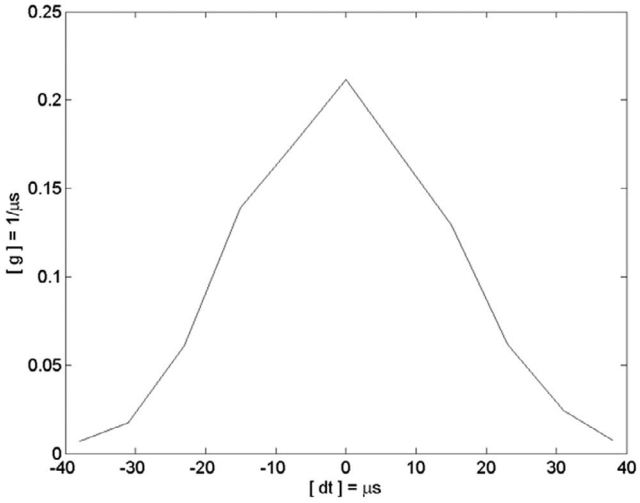

Figure 10. The timing accuracy of the ELF network of four instruments is ~30 μs as indicated by the distribution function g of the sum of arrival time differences calculated from the geolocation of ~680 lightning discharges observed between 28 and 30 August 2009.

Figure 2). This result means that any observed time of arrival differences >30 μs are physically meaningful and the result of ionospheric effects or the event properties. It is thus concluded that the worldwide ELF network can record, identify, and locate intense lightning discharges and sprites anywhere on planet Earth with a timing accuracy of ~30 μs.

6. Further Work

[30] Once the network has provided a suitable amount of data for analysis such as a more quantitative study of interesting individual events and a statistical analysis of time differences when compared to other more accurate VLF lightning networks, several options are available for improving the network. The first option is to use a higher sampling rate, which would add considerable high-frequency detail to the site nearest to any event. The limitations of this approach are that the remote sites would not benefit greatly, the maximum sampling rate would be constrained by the USB hard drive size, and the frequency with which the drives need to be swapped would increase. Another option is to add a computer to the nearest site in Eskdalemuir which would process data locally and provide a real-time data stream of sprites as they occurred. This real-time analysis could then be added to all sites and would help to identify sprite generating thunderstorms around the globe as they occur. An automated messaging system could inform optical sprite observers via e-mail or mobile phone if a sprite producing thunderstorm is occurring in their vicinity. In the more distant future, it would greatly enhance the network capability to add two further stations, one in South America and another in northern Japan. These two stations would help to identify the double peak from the causative lightning discharge and from the sprite more clearly using recordings made at the two nearest stations. Analytical methods used in other work using single instruments could also be used to enhance the capabilities of the network without additional hardware [*Ogawa and Komatsu*, 2010].

[31] **Acknowledgments.** This research was sponsored by the Science and Technology Facilities Council under grant PP/E0011483/1. The network could not have been created without the support of the South African Astronomical Observatory (SAAO), British Geological Survey (BGS), Geoscience Australia, and the University of California, San Diego, in hosting and maintaining the instruments at their observatory sites. Thanks also go to the engineers at Metronix/Coopertools for their invaluable technical support for the instruments. A number of people have lent their assistance to this project either technically or by providing sprite observations. Thanks to Oscar van der Velde, Oliver Chanrion, Serge Soula, Torsten Neubert, Steven Constable, and Hans-Werner Braun.

References

Boccippio, D. J., E. R. Williams, S. J. Heckman, W. A. Lyons, I. T. Baker, and R. Boldi (1995), Sprites, ELF transients, and positive ground strokes, *Science*, *269*, 1088–1091, doi:10.1126/science.269.5227.1088.

Boeck, W. L., O. H. Vaughan Jr., R. J. Blakeslee, B. Vonnegut, M. Brook, and J. McKune (1995), Observations of lightning in the stratosphere, *J. Geophys. Res.*, *100*(D1), 1465–1475, doi:10.1029/94JD02432.

Chen, A. B., et al. (2008), Global distributions and occurrence rates of transient luminous events, *J. Geophys. Res.*, *113*, A08306, doi:10.1029/2008JA013101.

Cummer, S. A., and U. S. Inan (2000), Modeling ELF radio atmospheric propagation and extracting lightning currents from ELF observations, *Radio Sci.*, *35*(2), 385–394, doi:10.1029/1999RS002184.

Cummer, S. A., U. S. Inan, T. F. Bell, and C. P. Barrington-Leigh (1998), ELF radiation produced by electrical currents in sprites, *Geophys. Res. Lett.*, *25*, 1281–1284, doi:10.1029/98GL50937.

Cummer, S. A., and M. Stanley (1999), Submillisecond resolution lightning currents and sprite development: Observations and implications, *Geophys. Res. Lett.*, *26*, 3205–3208, doi:10.1029/1999GL003635.

Cummer, S. A., H. U. Frey, S. B. Mende, R. Hsu, H. Su, A. B. Chen, H. Fukunishi, and Y. Takahashi (2006), Simultaneous radio and satellite optical measurements of high-altitude sprite current and lightning continuing current, *J. Geophys. Res.*, *111*, A10315, doi:10.1029/2006JA011809.

Franz, R. C., R. J. Nemzek, and J. R. Winckler (1990), Television image of a large electrical discharge above a thunderstorm system, *Science*, *249*, 48–51, doi:10.1126/science.249.4964.48.

Füllekrug, M. (2006), Elementary model of sprite igniting electric fields, *Am. J. Phys.*, *74*(9), 804–805, doi:10.1119/1.2206573.

Füllekrug, M., and S. Constable (2000), Global triangulation of intense lightning discharges, *Geophys. Res. Lett.*, *27*, 333–336, doi:10.1029/1999GL003684.

Füllekrug, M., D. R. Moudry, G. Dawes, and D. D. Sentman (2001), Mesospheric sprite current triangulation, *J. Geophys. Res.*, *106*(D17), 20,189–20,194, doi:10.1029/2001JD900075.

Füllekrug, M., E. Mareev, and M. Rycroft (Eds.) (2006), *Sprites, Elves and Intense Lightning Discharges*, *NATO Sci. Ser. II*, vol. 225, Springer, Dordrecht, Netherlands, doi:10.1007/1-4020-4629-4.

Huang, E., E. Williams, R. Boldi, S. Heckman, W. Lyons, M. Taylor, T. Nelson, and C. Wong (1999), Criteria for sprites and elves based on Schumann resonance observations, *J. Geophys. Res.*, *104*(D14), 16,943–16,964, doi:10.1029/1999JD900139.

Ignaccolo, M., T. Farges, A. Mika, T. H. Allin, O. Chanrion, E. Blanc, T. Neubert, A. C. Fraser-Smith, and M. Füllekrug (2006), The planetary rate of sprite events, *Geophys. Res. Lett.*, *33*, L11808, doi:10.1029/2005GL025502.

Lyons, W. A. (1996), Sprite observations above the U.S. High Plains in relation to their parent thunderstorm systems, *J. Geophys. Res.*, *101*(D23), 29,641–29,652, doi:10.1029/96JD01866.

Marshall, R. A., and U. S. Inan (2006), High speed measurements of small-scale features in sprites: Sizes and lifetimes, *Radio Sci.*, *41*, RS6S43, doi:10.1029/2005RS003353.

Neubert, T., et al. (2008), Recent results from studies of electric discharges in the mesosphere, *Surv. Geophys.*, *29*(2), 71–137, doi:10.1007/s10712-008-9043-1.

Ogawa, T., and M. Komatsu (2007), Analysis of *Q* burst waveforms, *Radio Sci.*, *42*, RS2S18, doi:10.1029/2006RS003493.

Ogawa, T., and M. Komatsu (2010), Propagation velocity of VLF-EM waves from lightning discharges producting Q-bursts observed in the range 10–15 Mm, *Atmos. Res.*, *95*, 101–107, doi:10.1016/j.atmosres.2009.08.015.

Parkinson, B. W., and J. J. Spilker (1996), *Global Positioning System: Theory and Applications*, vol. 1, Am. Inst. of Aeronaut. and Astronaut., Reston, Va.

Rakov, V. A., and M. A. Uman (2003), *Lightning Physics and Effects*, Cambridge Univ. Press, New York.

Reising, S. C., U. S. Inan, T. F. Bell, and W. A. Lyons (1996), Evidence for continuing currents in sprite-producing lightning flashes, *Geophys. Res. Lett.*, *23*(24), 3639–3642, doi:10.1029/96GL03480.

Rodger, C., N. Thomson, and J. Wait (1999), VLF scattering from red sprites: Vertical columns of ionization in the Earth ionosphere waveguide, *Radio Sci.*, *34*(4), 913–921, doi:10.1029/1999RS900051.

Rycroft, M. J. (1965), Resonances of the Earth-ionosphere cavity observed at Cambridge, England, *J. Res. Natl. Bur. Stand. U.S., Sect. D*, *69*, 1071–1081.

Rycroft, M. J., et al. (2007), New model simulations of the global atmospheric electric circuit driven by thunderstorms and electrified shower clouds: The role of lightning and Sprites, *J. Atmos. Sol. Terr. Phys.*, *69*, 2485–2509, doi:10.1016/j.jastp.2007.09.004.

Saba, M. M. F., W. Schulz, T. A. Warner, L. Z. S. Campos, C. Schumann, E. P. Krider, K. L. Cummins, and R. E. Orville (2010), High-speed video observations of positive lightning flashes to ground, *J. Geophys. Res.*, *115*, D24201, doi:10.1029/2010JD014330.

Sato, M., and H. Fukunishi (2003), Global sprite occurrence locations and rates derived from triangulation of transient Schumann resonance events, *Geophys. Res. Lett.*, *30*(16), 1859, doi:10.1029/2003GL017291.

Sentman, D. D., and E. M. Wescott (1993), Observations of upper atmospheric optical flashes recorded from an aircraft, *Geophys. Res. Lett.*, *20*, 2857–2860, doi:10.1029/93GL02998.

Taylor, W., and K. Sao (1970), ELF attenuation rates and phase velocities observed from slow-tail components of atmospherics, *Radio Sci.*, *5*(12), 1453–1460, doi:10.1029/RS005i012p01453.

Williams, E. R., et al. (2007), Sprite lightning heard round the world by Schumann resonance methods, *Radio Sci.*, *42*, RS2S20, doi:10.1029/2006RS003498.

A. Bennett, Passive Upper Air Sensors R&D, Meteorological Office, Devon EX1 3PB, UK.

J. Dyers, P. Fourie, and R. Sefako, South African Astronomical Observatory, Observatory Road 7825, Cape Town, South Africa.

D. Elliott and F. Wyatt, Scripps Institution of Oceanography, University of California, San Diego, La Jolla CA 92093-0225, USA.

S. Flower and A. Thomson, British Geological Survey, Edinburgh EH9 3LA, UK.

M. Füllekrug and T. Whitley, Department of Electronic and Electrical Engineering, University of Bath, Bath BA2 7AY, UK. (tw236@bath.ac.uk)

G. Heinson, School of Earth and Environmental Sciences, University of Adelaide, Adelaide, SA 5005, Australia.

A. Hitchman and A. Lewis, Geoscience Australia, GPO Box 378, Canberra, ACT 2601, Australia.

M. Rycroft, CAESAR Consultancy, 35 Millington Rd., Cambridge CB3 9HW, UK.